Efficient viral expression of a chemogenetic receptor in the old-world monkey amygdala

Walter Lerchner [a,*], Kiana Dash [a], Deborah Rose [a], Mark.A.G. Eldridge [a], Kathryn.M. Rothenhoefer [b], Xuefeng Yan [c], Vincent.D. Costa [b], Bruno Averbeck [a], Barry.J. Richmond [a,**]

[a] Laboratory of Neuropsychology, National Institute of Mental Health, National Institutes of Health, Bethesda, MD, 20892, USA
[b] Division of Neuroscience, Oregon National Primate Research Center, Oregon Health and Science University, Beaverton, OR, USA
[c] Molecular Imaging Branch, National Institute of Mental Health, National Institutes of Health, Bethesda, MD, USA

ABSTRACT

Genetically encoded synthetic receptors, such as the chemogenetic and optogenetic proteins, are powerful tools for functional brain studies in animals. In the primate brain, with its comparatively large, intricate anatomical structures, it can be challenging to express transgenes, such as the hM4Di chemogenetic receptor, in a defined anatomical structure with high penetrance. Here, we compare parameters for lentivirus vector injections in the rhesus monkey amygdala. We find that four injections of 20 μl, infused at 0.5 μl/min, can achieve neuronal hM4Di expression in 50–100% of neurons within a 60 mm^3 volume, without observable damage from overexpression. Increasing the number of hM4Di_CFP lentivirus injections to up to 12 sites per hemisphere, resulted in 30%–40% neuronal coverage of the overall amygdala volume, with coverage reaching 60% in some subnuclei. Manganese Chloride was mixed with lentivirus and used as an MRI marker to verify targeting accuracy and correct unsuccessful injections in these experiments. In a separate monkey we visualized, in vivo, viral expression of the hM4Di receptor protein in the amygdala, using Positron Emission Tomography. Together, these data show efficient and verifiable expression of a chemogenetic receptor in old-world monkey amygdala.

1. Introduction

Of all anatomical structures in the mammalian brain, the amygdala might be the most fascinating but also one of the most challenging regions to characterize (Phelps and LeDoux, 2005; Janak and Tye, 2015; Murray and Fellows, 2022). While relatively easy to localize by its almond-shape and its central position in anterior temporal lobe, it comprises several distinct subnuclei whose molecular and functional characteristics are actively studied and debated (Roozendaal et al., 2009; Kim et al., 2017; Wank et al., 2021). Efficiently targeting subnuclei of the amygdala with genetically encoded receptors and reporters will give researchers powerful tools to further study the function and neural circuit of these structures.

Several recent studies virally expressed chemogenetic receptors in the monkey amygdala using Adeno-associated virus with an AAV5 serotype (Grayson et al., 2016; Kalin et al., 2016; Raper et al., 2019; Roseboom et al., 2021), and showed metabolic (Grayson et al., 2016), physiological (Kalin et al., 2016) and/or behavioral effects (Raper et al., 2019; Roseboom et al., 2021). Subsequent histological examination of

the injection sites within the amygdala showed large variations in efficiency of cellular and regional targeting, with little to no expression in the central nucleus of the amygdala in adolescent/young monkeys (Kalin et al., 2016; Roseboom et al., 2021) and adult monkeys (Grayson et al., 2016). However, AAV5 serotype was used to express a chemogenetic receptor in specific neuron populations in the mouse amygdala (Wank et al., 2021), suggesting an interspecies difference in viral tropism. One reason for the variability might be idiosyncrasies of AAV serotypes, resulting in heterogeneous expression in different neuron populations, something generally not seen with lentivirus vectors with the VSV-G glycoprotein (Jazayeri et al., 2012; Lerchner et al., 2014).

Another challenge with comprehensively targeting a relatively large and irregular structure, such as the amygdala, is that it requires multiple penetrations to accurately infuse the virus deep below the cortical surface (Lerchner et al., 2023). Thus, it is advantageous to visualize the successful infusion of the virus as well as the subsequent expression of the desired protein in the living monkey before further experiments are initiated. One method to monitor correct targeting is to co-infuse the virus with the MRI marker Gadolinium (Fiandaca et al., 2009), but

---

Gadolinium diffuses within one or two hours of injection (Lin and Brown, 2007). Therefore, Gadolinium is most useful for this purpose when injection is monitored during the surgery, allowing live monitoring of flow (Fiandaca et al., 2009), but is problematic for in vivo verification after longer surgeries. Another option for in vivo verification of injections is Manganese ions (Mn^{2+}), delivered in the form of salts, dissolved and mixed with the virus prior to infusion (Fredericks et al., 2020; Lerchner et al., 2023). Mn^{2+} signal can be detected locally for hours after surgery before it starts to travel along axon projections (Simmons et al., 2008; Fredericks et al., 2020).

Here, we show that we can efficiently express the hM4Di_CFP DREADD (Eldridge et al., 2016) from a lentivirus in various subnuclei of the amygdala by multiple injections of 20 μl of virus suspension at speeds of 0.5 μl per minute. In addition, we show that mixing of up to 10 mM of $MnCl_2$ with the lentivirus does not appear to adversely affect titer and that we can use Positron Emission Tomography to verify the correct location of the chemogenetic receptor expression in the amygdala in the living monkey six weeks after injection.

2. Materials/methods

2.1. Subjects

We used 4 male rhesus monkeys (8–10 kg) for this study. Experimental procedures followed the Institute of Laboratory Animal Research Guide for the Care and Use of Laboratory Animals and were approved by the National Institute of Mental Health Animal Care and Use Committee.

2.2. Lentivirus vector construction and production

The viral vector LV-hM4Di_CFP was produced by packaging the pLenti-hSYNhM4Di_CFP-WPRE plasmid (Eldridge et al., 2016) with the VSV-G capsid protein in 293T kidney cells as described in detail previously (Fredericks et al., 2020). Concentrated lentivirus particles were suspended in PBS and stored at −80 °C in 10 μl aliquots.

2.3. Determining lentivirus titer for surgeries and time course experiments

Lentivirus aliquots were thawed on ice and 3 μl of virus was used to transduce wells of 1.5×10^5 293T cells that were allowed to multiply to approximately 10^6 cells before the DNA were harvested 48 h later. A qPCR Lentivirus Titer Kit (ABM, LV900) was used to compare amplification of viral DNA to amplification of an endogenous gene (hVAR). See (Lerchner et al., 2023) for a detailed description of the procedure. For surgeries and as a starting point for the time course experiment, virus titers were adjusted to 2×10^9 iu/ml with cold PBS after thawing virus aliquots.

2.4. Lentivirus titer time course experiment

Virus aliquots were thawed on ice and cold PBS was added to adjust the titer to 2×10^9 iu/ml. Then sufficient virus sample for each time series was either kept on ice for the 4 °C control or mixed with $MnCl_2$ or Gadolinium and loaded into a 100 μl Hamilton syringe. At each time point 10 μl was expelled and duplicates were transduced with 293T cells for each series as described above for determining infectious units (iu). Similarly, 10 μl of virus suspension was taken from the control sample kept on ice at each time point.

2.5. Virus injections

Surgical procedures were performed in a veterinary operating facility under aseptic conditions. Vital signs were monitored throughout the procedure. A pre-operative T1-weighted magnetic resonance imaging (MRI) scan for each monkey was used to determine the stereotaxic coordinates for the sites of the lentivirus injection in each amygdala. The skull region above the target site was exposed by retracting the skin, fascia, and muscle in anatomical layers. A small boneflap was then removed (~1.5 cm diameter) to access the dura mater, into which incisions were made to provide access for the injection apparatus (Fredericks et al., 2020). Lentivirus with a titer of 2×10^9 iu/ml was loaded into a 100 μl glass syringe (Hamilton Co., MA). The 30-gauge needle of the syringe was sheathed with a silica capillary (450 μm OD) to create a step 1 mm from the base of the aperture. The syringe was mounted in a Nanomite pump (Harvard Apparatus, Cambridge, MA). The needle was lowered through the incision in the dura mater to each of the pre-calculated target sites and the virus suspension was infused at a rate of 0.5 μl per min. After each injection, the needle was left at the position for 10 min after each injection to allow pressure to dissipate. The needle was then slowly removed. At the completion of the injection series the soft tissues were sutured together in anatomical layers.

2.6. Magnetic resonance imaging

Magnetic resonance imaging (MRI) scan were performed after brain injection using a 3T MRI scanner (Achieva dStream, Philips Healthcare, Best, Netherlands), as described in detail (Fredericks et al., 2020). For post-op MRI procedures, anesthesia was prolonged with ketamine (5 mg/kg, i.m.). An additional dose of Ketamine was given before the scan, if required.

2.7. Immunohistochemistry

At a minimum of 6 weeks following the injections, the monkeys were deeply anesthetized with Beuthanasia solution and perfused with 1 L of normal saline solution followed by 3 L of 4% paraformaldehyde in 0.1M PBS. The brains were removed and cryoprotected through a series of glycerols in 0.1M PBS. The brains were blocked in the coronal plane and then quickly frozen in −80 °C isopentane. The brain was cut into 40 μm slices along the coronal plane and the sections were collected in 10 series. For histochemistry, sections were blocked in 5% normal goat serum and 0.3%Triton-X 100 in tris-buffered saline (TBS), incubated with primary antibody in blocking buffer, washed and, incubated with an horse radish peroxidase secondary antibody (Vector labs, Burlingame, CA, USA, PI-1000) for 90 min and visualized with a 3,3′-diaminobenzidine (DAB) reaction (Lerchner et al., 2014). For immunofluorescence secondary rabbit and mouse antibodies were purchased from Molecular Probes (Life Technologies), spectra as indicated in the figure legends. The secondary antibody for fluorescence detection of chick anti GFP was purchased from Abcam (DyLight 488 goat anti-Ch - ab96947).

2.8. Cell counting and 3D reconstruction

Following image collection, the sections were aligned and compiled into stacks using BrainMaker (MBF Bioscience), with 400 μm between sections. A stack was created for each brain hemisphere of each monkey. The image stacks were then imported into Nuerolucida360 (MBF Bioscience) for analysis. The amygdala as well as expression regions were outlined by utilizing Contour mode of the program. Area measurements were calculated from these outlines by the program. While only visualizing either the GFP of NeuN channel, photoshop counters were used to mark and categorize positive cells. For establishing cell counts, the expression areas were overlaid with a 100 μm × 100 μm grid and counts for each grid transferred into a corresponding grid table in Microsoft Excel. This process was repeated for all sections within the stacks. 3D reconstructions of each brain hemisphere were created using the 3D environment of Neurolucida360 to visualize the viral expression in the monkey amygdala.

2.9. PET scanning and image processing

For each radioligand, six scans (three baseline and three blocked)

were performed in a single monkey using a microPET Focus 220 scanner (Siemens Medical Solutions; Knoxville, TN). Baseline scans were performed in the morning and blocked scans were performed in the afternoon of the same day. The interval between imaging sessions was at least three weeks. The weight of the animal varied little during the total period of the studies (body weight = 11.6 ± 0.9 kg). PET images were acquired after injection of [11C]CLZ (278 ± 64 MBq) or [11C]DCZ (302 ± 51 MBq) for 2 h, with frame duration ranging from 30 s to 10 min. For all PET imaging procedures, anesthesia was induced with ketamine (10 mg/kg, i.m.) and then maintained with 1–2% isoflurane and 98% O2. PET imaging data were reconstructed using Fourier rebinning plus two-dimensional filtered back-projection with attenuation and scatter correction. Images were co-registered to a standardized monkey MRI template using PMOD software (PMOD Technologies, LLC, Zurich, Switzerland). Thirty-five predefined brain regions of interest from the template were applied to the co-registered PET image to obtain regional time-activity curves. The target (DREADD) region was drawn manually based on post-operative MRI. Brain uptake was expressed as standardized uptake value (SUV), which normalizes for injected radioactivity and body weight (Yan et al., 2021).

3. Results

3.1. Lentivirus injections into the amygdala

The lentivirus construct expressing the hM4DI_CFP fusion protein under the control of a 400 bp neuron specific promoter

(hSYNhM4Di_CFP) was packaged into lentivirus vector particles and injected into both hemispheres of the monkey amygdala (Fig. 1A). In the right hemisphere, 80 μl of virus suspension (2 × 10E9 iu/ml) was infused into a single location. In the left hemisphere the same total amount of the suspension was injected in four infusions of 20 μl set on the corners of a 2 mm wide square (Fig. 1A).

Enzymatic staining using an anti-GFP antibody revealed strong expression throughout the amygdala (Am) in both hemispheres (Fig. 1B). Staining was also present in regions receiving projections from the amygdala, such as the preoptic area of the hypothalamus (labeled Po) and the Rhinal Cortex (labeled Rh). This is expected because the hM4Di_CFP protein is transported from the cell body into axons. Cell body (somatic) expression, visualized with single cell resolution confocal microscopy, was much more confined, mostly to regions in the central and dorsomedial portions of the amygdala (Fig. 1C). Somatic expression was observed in slices through 4 mm of the amygdala (Fig. 1D). The outline of regions of receptor expression was irregular for both types of injections. This is likely because of the diffusion of vector particles along structural boundaries (e.g. white matter tracts between basal and central regions) and along blood vessels (Lentz et al., 2012).

3.2. 20 μl injections of lentivirus into amygdala result in high neuronal coverage

To analyze expression coverage using confocal microscopy, we imaged a series of fluorescently stained sections for co-expression of CFP and the neuronal marker NeuN (Fig. 2A and B) and outlined the
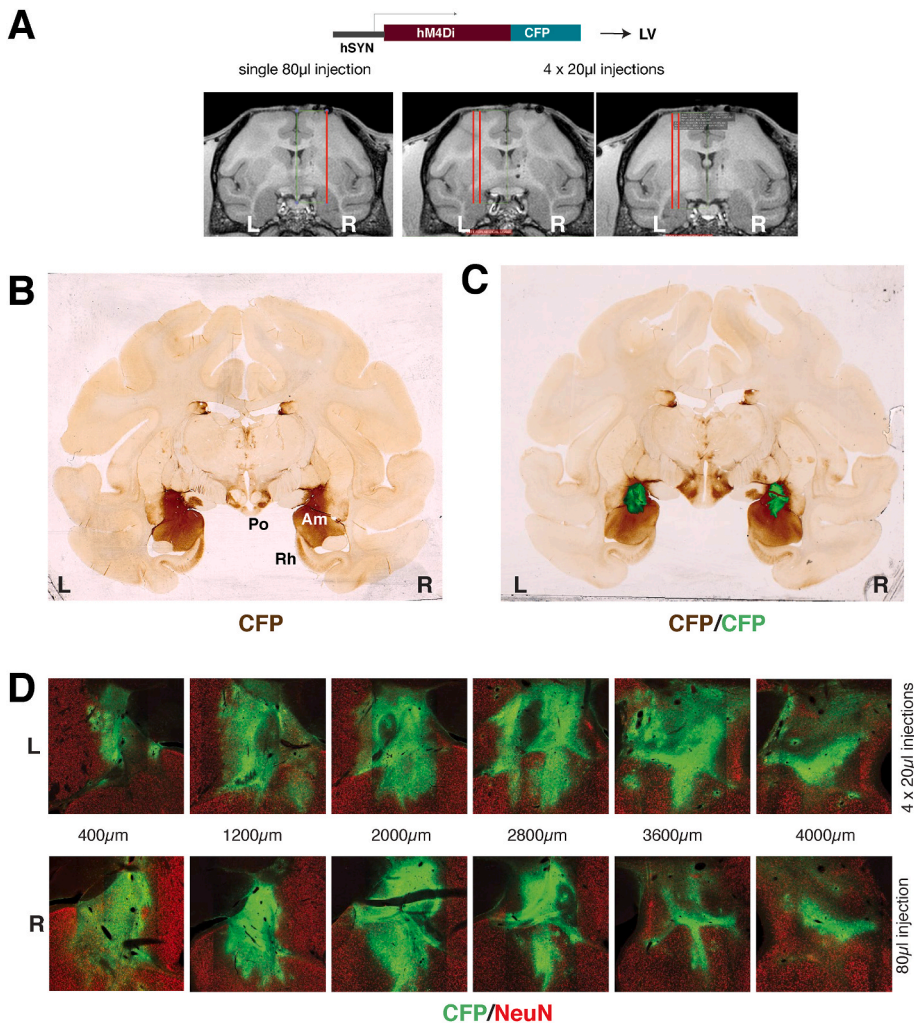

Fig. 1. Vector mediated hM4Di_CFP (DREADD) fusion gene expression in the amygdala. A. The human synapsin promoter construct expressing the hM4Di_CFP protein was packaged into Lentivirus (LV) vector. MRI with intended injection tracks overlaid as red line. Right side received a single injection of 80 μl. Left side (L) received 4 injections of 20 μl each, in a square pattern, approx. 2 mm apart. B. DAB visualization of LV- hM4Di_CFP. Am: Amygdala, Po: Preoptic nucleus of the hypothalamus, Rh: Rhinal cortex. C. DAB visualization of hM4Di_CFP expression overlaid with fluorescent CFP signal from staining of an adjacent 40 μm section. D. Fluorescent confocal sections in 800 μm distance over the 4 mm expression areas from both sets of injections. (For interpretation of the references to color in this figure legend, the reader is referred to the Web version of this article.)
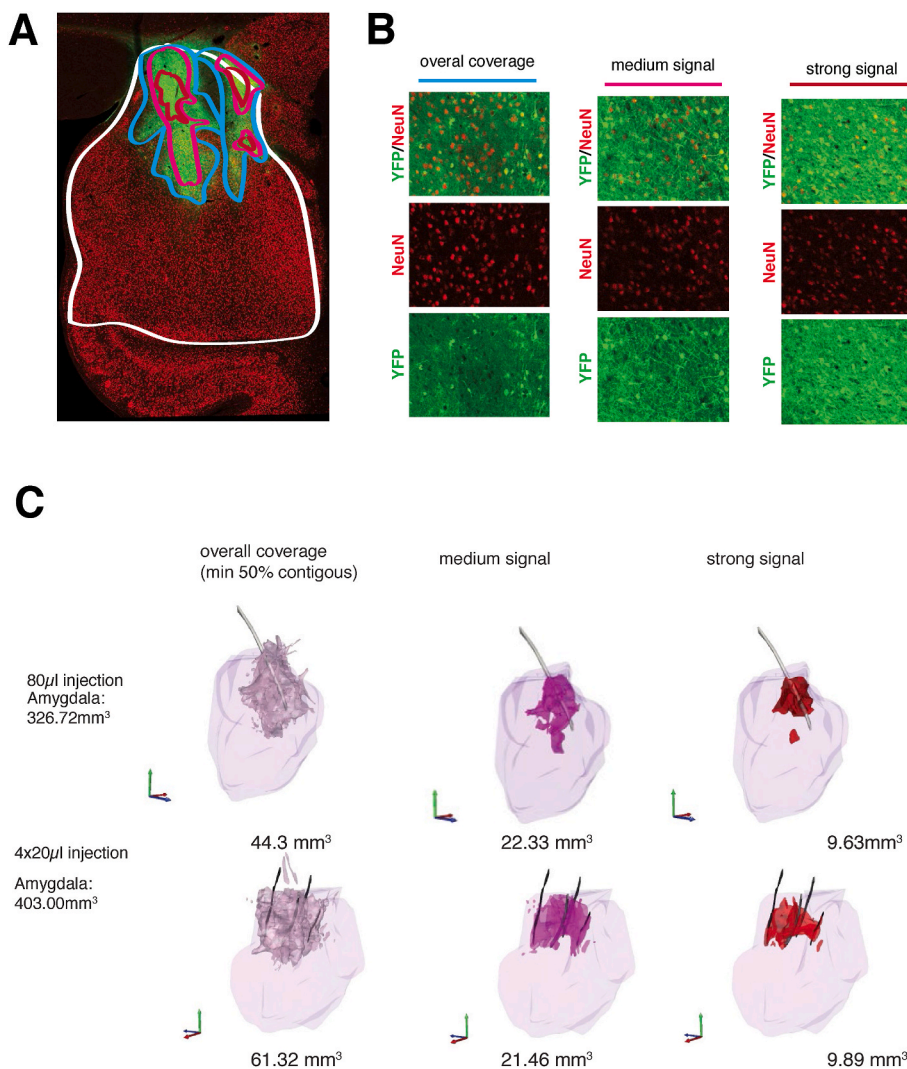
Fig. 2. Outlining of somatic hM4Di_CFP expression areas on confocal sections. A. Amygdala is outlined in white. Blue: Overall expression areas. Pink: Areas with medium signal (90–100% penetrance). Dark Red: strong signal (100 penetrance). **B.** Higher magnification taken from samples of outlined expression areas. **C.** 3D reconstruction models of expression in the context of the amygdala. Amygdala region is visualized as a translucent purple sphere. Reconstructed injection tracts are visualized as gray cylindrical straws. hM4Di_CFP expression is shown in solid colors. (For interpretation of the references to color in this figure legend, the reader is referred to the Web version of this article.)

boundaries of the amygdala in white (Fig. 2A). We then traced outlines around areas with contiguous somatic expression for three intensities as agreed upon by independent observers: To designate regions of *overall coverage*, outlines were traced around areas in which at least 50% of neurons were positive for hM4Di_CFP, with a minimum of 10 neurons total in each outlined area (Fig. 2 A, B, blue trace). As shown in Fig. 2A, within areas of overall coverage, we then outlined areas with *medium signal* (at least 90%–100% of NeuN cells express hM4Di_CFP – pink trace) and strong signal (100% of NeuN positive cells express hM4Di_CFP at high intensity – dark red trace). Outlined areas were then aligned within the Neurolucida software (MBF Bioscience, Vt, USA). Expression volumes were reconstructed and visualized in 3D (Fig. 2C). Volumes of strong and medium signal were nearly identical in both hemispheres (approx. 10 mm^3 and 20 mm^3, respectively) but the overall volume of amygdala expression (at least 50% of neurons expressing) was substantially larger for the 4 × 20 μl injections than for the single 80 μl injection (Fig. 3C).

3.3. 20 μl lentivirus injections have higher density of coverage with less neuronal damage

Some physical damage resulting in loss of neurons within the injected regions is expected because of needle damage (white outline in Fig. 3A). For the 80 μl injection on the right side, we also detected regions with dense expression of hM4Di_CFP that corresponded with a complete shut-down of NeuN (brown outline in Fig. 3A), suggesting that overexpression of the virus could affect neuronal integrity, a result consistent with previously reported over-expression effects (Guselnikova and Korzhevskiy, 2015).

Overlaying a grid of 100 μm × 100 μm squares onto the expression areas on each section (Fig. 3B, left panel), we counted the percentage of hM4Di_CFP expressing neurons within each square, i.e., neurons that showed somatic expression of both hM4Di_CFP and NeuN vs. neurons only expressing the NeuN marker protein (Fig. 3B, middle panel) from which we calculated the percentage of CFP positive neurons in each square (Fig. 3B, right panel). Fig. 3C shows an example of hM4Di and NeuN expression within a square. A histogram for the frequency of squares with neuronal coverage from 10% to 100% is depicted in Fig. 3D. The four injections of 20 μl each, not only covered a larger area than the single large injection, but also produced more regions with high percentages of neuronal coverage within the expression regions: in 57% of the expression region more than 80% of neurons were positive for DREADD expression, and an additional 17% of squares had expression in more than 70% of neurons. That compared to 50% and 12%, respectively, for the single 80 μl injection. The distribution of expression intensity of the 4 × 20 μl injections (Fig. 3D) indicated a sharper boundary around the expression region, with fewer of the squares showing expression of less than 60% compared with the 80 μl injection.

The overall expression volume of the single 80 μl injection covered a region of 44 mm^3 compared to an overall expression volume of 61 mm^3
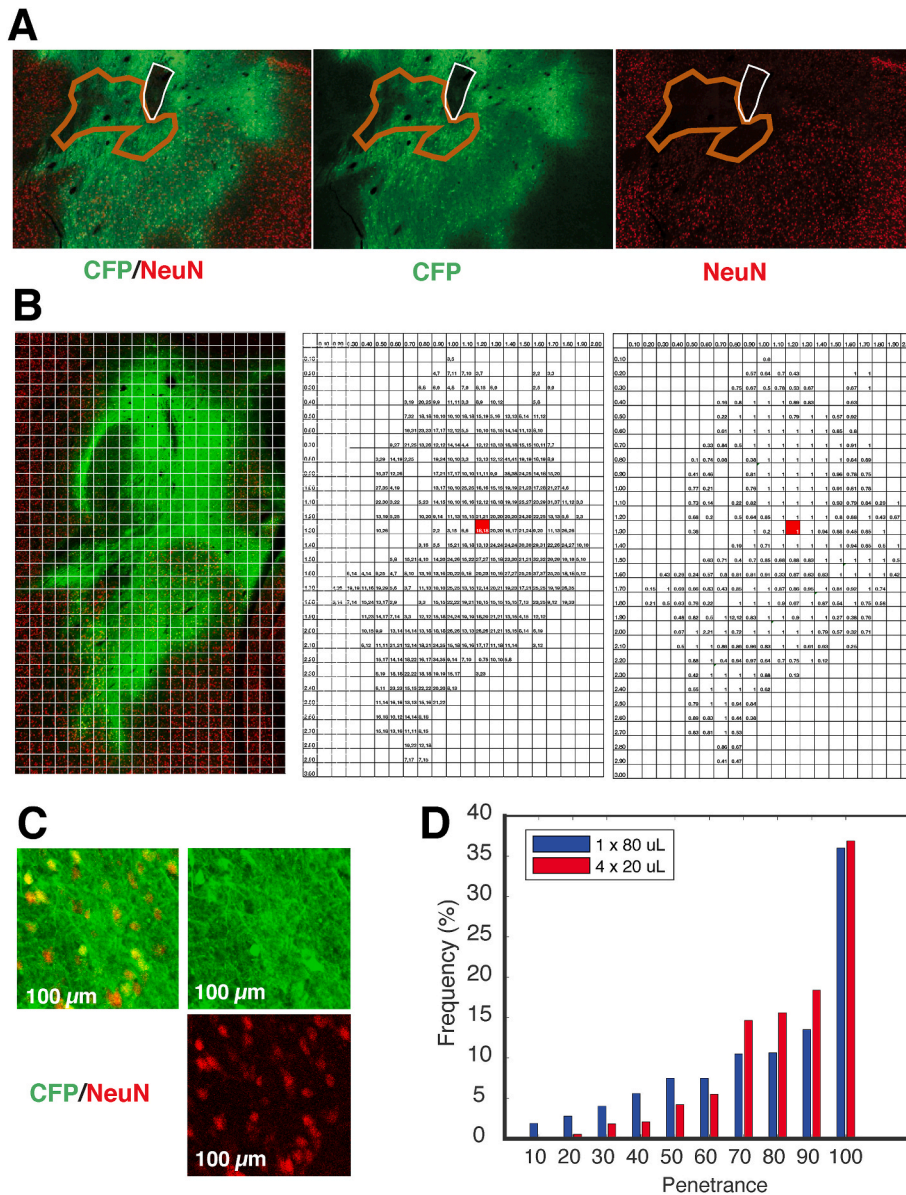
Fig. 3. 20 μl injections have tighter expression boundaries, while 80 μl injection results in regions with NeuN shut-down. A. Red outline of region with CFP signal but no NeuN. White outline for region with cellular damage, presumably from the needle tract. **B.** Example for the 100 μm × 100 μm square grid overlayed onto a slide with the 80 μl injection (right panel). Middle panel: Each square contains the number of CFP expressing neurons, followed by the total number of neurons in each square. Right panel: Each grid cell contains the fraction of CFP expressing neurons over the total number of neurons in each cell. The red grid cell indicated the location of the injection site. **C.** Example for CFP and NeuN staining within a grid cell at 10× magnification. **D.** Histogram of frequency of LV-hM4Di_CFP expressing regions over neuronal penetrance. (For interpretation of the references to color in this figure legend, the reader is referred to the Web version of this article.)

for the four 20 μl injections, i.e. the four injections covered approximately 38% more volume of somatic expression (Table 1). Volumes for strong and medium signal outlines were similar for both types of injections (10 mm^3 and 22 mm^3 respectively) but the single 80 μl injection also showed nearly 5% of volume (2.2 mm^3) with damage or complete down-regulation of NeuN signal (Fig. 5), likely due to toxicity of hM4Di_CFP overexpression. No NeuN down-regulation was observed for the 4 × 20 μl injections, and no damage was detected beyond that caused

by the mechanical insertion of the four needles. These results gave us confidence that a larger series of 20 μl injections could be used to cover larger regions, such as the whole volume of the amygdala, at neuronal penetrance of 50%–100% with minimal neural damage.

3.4. Lentivirus is stable for at least 6 h at room temperature

In the experiment described above, injections of 4 × 20 μl of virus covered a volume of approximately 60 mm^3. A typical old world monkey amygdala has a volume of approximately 300 mm^3 (Zhao et al., 2013). Thus, coverage of the entire amygdala will require a scaling up of the number of injections, resulting in virus potentially being held in the syringe or a reservoir for multiple hours at room temperature (Fredericks et al., 2020). To test the lentivirus stability over time, we loaded a 100 μl syringe with freshly thawed and diluted LV-hM4Di_CFP (2 × 10E9 IU/ml), and expelled 10 μl of virus into wells of cultured cells, at time points from 0 to 6 h (Fig. 4A). As a control, we analyzed 10 μl aliquots taken from virus samples kept on ice, at the same time points. The act of taking up the virus into the syringe and expelling it consistently reduced the titer by about 30% compared to the sample kept on ice. Both the syringe sample and the sample kept on ice showed a reduction of
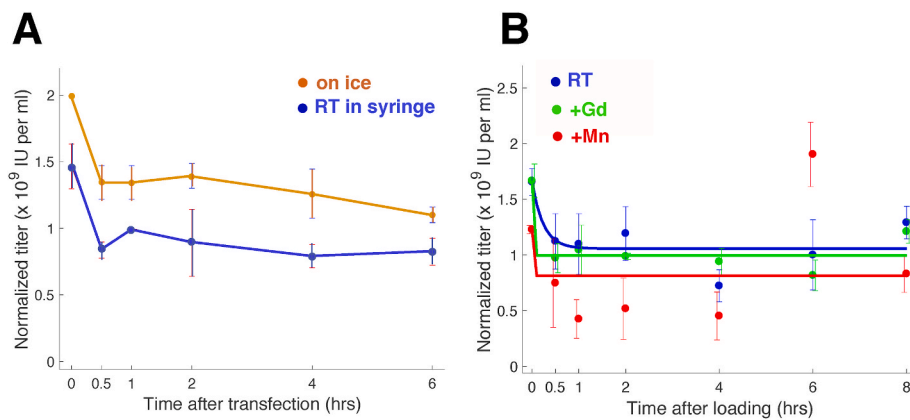
Table 1
Summary of reconstructed regions from outlined expression regions.

	1 × 80 μl Injection		4 × 20 μl Injection	
	Volume (mm^3)	% of Overall Coverage	Volume (mm^3)	% of Overall Coverage
Overall Coverage	44.33	100.00%	61.32	100.00%
Medium Signal	22.33	50.38%	21.46	35.00%
Strong Signal	9.63	21.72%	9.89	16.12%
Damaged Region	0.63	1.42%	0.87	1.42%
Region with NeuN shutdown	1.63	3.68%	N/A	N/A

Fig. 4. A. Time course to test for Lentivirus (LV) stability. orange line: LV-hM4Di_CFP kept on ice after thawing. Blue line: LV- hM4Di_CFP taken up in a syringe at room temperature (RT) and expelled in 10 μl aliquots at time points indicated. **B.** Time course to test for LV stability at room temperature when combined with MRI markers Gadolinium or MnCl₂. Blue line: LV- hM4Di_CFP in PBS. Green line: LV-hM4Di_CFP with 1 mM Gadolinium (+Gd). Red line: LV-hM4Di_CFP with 10 mM MnCl₂ (+Mn). (For interpretation of the references to color in this figure legend, the reader is referred to the Web version of this article.)
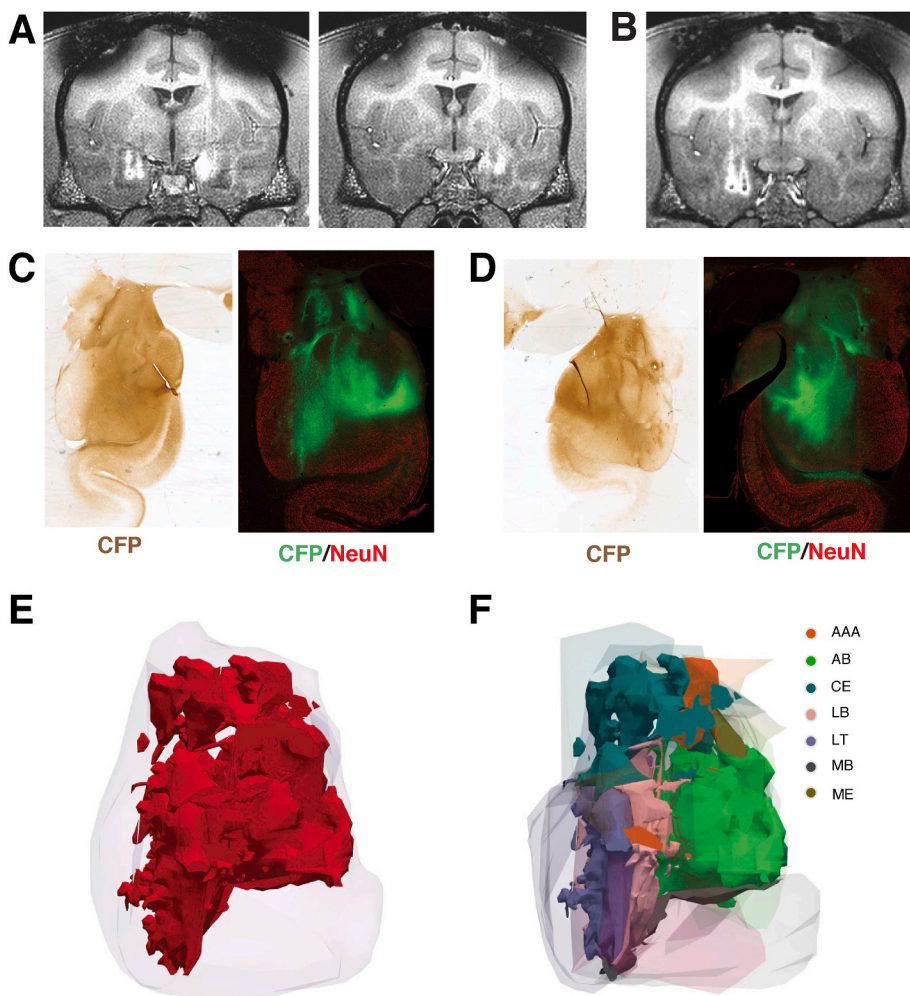

Fig. 5. Injection of LV-hM4Di_CFP to target the amygdala bilaterally. A. MRI 4 h after surgery. Mn^{2+} hypersignal is white. **B.** MRI after re-injection of LV- hM4Di_CFP in 2 addition tracks (5 injections). **C.** Signal in the left amygdala against LV-hM4Di_CFP with DAB (left panel) and confocal visualization against CFP (green) and NeuN (red) (right panel). **D.** Signal in the right amygdala against LV-hM4Di_CFP with DAB (left panel) and confocal visualization against CFP (green) and NeuN (red) (right panel). **E.** 3D reconstruction of overall cell body expression (>50%) in the context of the amygdala. Amygdala is visualized in translucent purple. hM4Di_CFP expression is visualized in solid red. **F.** 3D reconstruction of overall cell body expression (>50%) in the context of amygdala subnuclei. Subnuclei are visualized in translucent colors. hM4Di_CFP expression is visualized in solid colors. AAA: Anterior Amygdaloid Area, AB: Accessory Basal Nucleus, CE: Central Nucleus, LB: Lateral Basal Nucleus, LT: Lateral Nucleus, MB: Medial Basal Nucleus, ME: Medial Nucleus. (For interpretation of the references to color in this figure legend, the reader is referred to the Web version of this article.)

virus titer by about 30% within the first 30 min but no further reduction of virus titer between 30 min and 6 h. These results indicated that using 100 μl syringes pre-loaded with lentivirus should be suitable for large volumes of injections.

3.5. Addition of the MRI marker MnCL₂ does not affect lentivirus titer

From the results discussed above, we concluded that multiple 20 μl injection volumes of LV-hM4Di_CFP should give us the best chance of maximizing coverage in the amygdala without causing damage from overexpression. To cover the entire volume of the amygdala, we estimated that we needed 15 or more individual injections of 20 μl. This brings with it a significant danger of injections failing (e.g., because of needle blockage) or being mis-targeted (e.g., because of needle deflection). To verify flow and accuracy of injections, an MRI contrast agent can be added to the virus mixture (Fredericks et al., 2020). To test whether the MRI contrast agents Gadolinium (Gd) or Manganese Chloride (MnCl₂) would adversely affect titer in the time span of a surgery, we repeated cell culture assay with the addition of either 10 mM MnCl₂ or 1 mM Gd. Mixing LV-hM4Di_CFP with Gd or Mn^{2+}, and expelling

samples from a syringe, did not appear to affect virus titers compared to a LV-hM4Di_CFP control (Fig. 4B). The addition of 10 mM MnCl$_2$ appeared to make the titers more variable, possibly because of a tendency for the virus to aggregate at this relatively high MnCl$_2$ concentration. Using trial and error in subsequent experiments, we found that the risk of aggregation can be reduced by allowing the virus sample to equilibrate to room temperature before mixing in the MnCl$_2$. For in vivo studies, we recommend injecting Mn at a final concentration if 0.1–0.5 mM; at these low concentrations we rarely observe the formation of any precipitate.

3.6. Bilateral injections of LV-hM4Di_CFP into the amygdala

Extrapolating from the four 20 μl lentivirus injections, we injected a pilot monkey with 12 × 20 μl of LV-hM4Di_CFP into each hemisphere with 6 needle tracks and 2–3 injections per track spaced 1.5–2 mm apart on the ventral/dorsal axis. We mixed MnCl$_2$ with the lentivirus to visualize injection sites but reduced the concentration to 0.5 mM, which resulted in strong hypersignals in the MRI scan following the surgery (Fig. 5A). Two of the tracks on the left side did not show signal, likely due to needle blockage. The injection procedure was repeated for these tracks in a second surgery two weeks later. In the MRI visualization following surgery both repeat injections resulted in a clear signal for all injections (Fig. 5B). When the brain was analyzed post-extraction,

enzymatic staining resulted in strong signal in the amygdala of both hemispheres. Confocal fluorescent visualization of cell bodies showed that the signal was confined to the amygdala, but did not cover all regions equally (Fig. 5C and D). We outlined contiguous regions with at least 50% neuronal penetrance and created a 3D model of the expression in the context of the amygdala (Fig. 5E). We also outlined the major subnuclei in a second 3D model (Fig. 5F). Analysis of the outlines with MBF Neurolucida showed that we achieved an overall coverage of 42% for the left amygdala and 32% for the right amygdala, with coverage reaching more than 60% for some of the nuclei, such as the Lateral Basal nucleus (LB) on the left (Fig. 6B) and the Anterior Amygdala Area (AAA) and the Accessory Basal nucleus (AB) on the right (Fig. 6B).

3.7. In vivo visualization of LV-DREADD expression in the amygdala

We previously showed that hM$_4$Di expression can be visualized in vivo using Positron Emission Tomography (Nagai et al., 2016; Yan et al., 2021). To test whether expression from multiple 20 μl injections in the amygdala can be detected in the living monkey, we infused 10 locations within the left amygdala (Fig. 7 left panel) and, after allowing at least six weeks for the protein to accumulate, imaged the hM$_4$Di expression with either radioactively labeled clozapine [11C]CLZ (Fig. 7 middle panel) or radioactively labeled [11C]DCZ (Fig. 7 right panel), an improved ligand with higher PET sensitivity (Yan et al., 2021; Oyama et al., 2022). Both
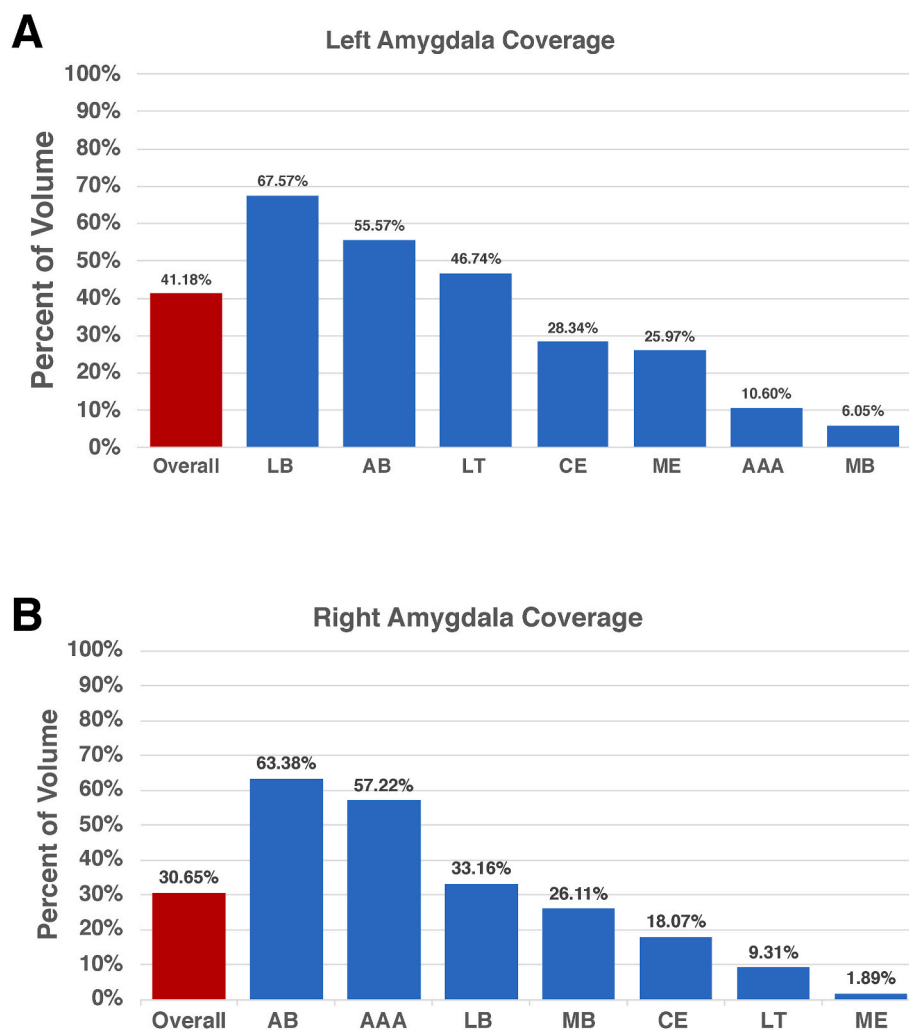

Fig. 6. Percentage of bilateral amygdala coverage. A. Coverage in amygdala and subnuclei in the left amygdala. **B.** Coverage in amygdala and subnuclei in the right amygdala. Legend: LB. lateral basal nucleus; LT. lateral nucleus; AB. Accessory basal nucleus; ME. medial amygdala; AAA. Anterior amygdaloid area; CE. central nucleus; MB. medial basal nucleus.
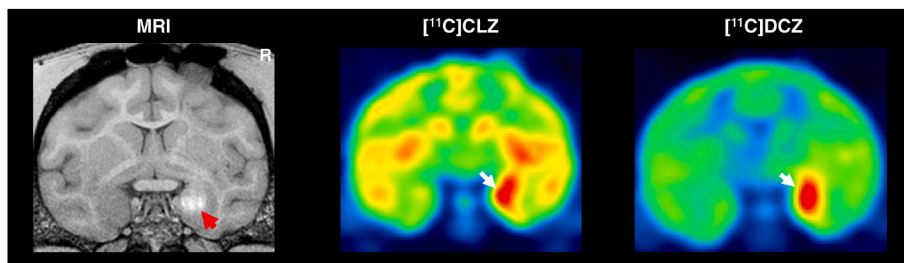
Fig. 7. PET imaging to visualize amygdala expression of hM4Di. Left panel: Mn^{2+} signal of lentivirus infusion into the left amygdala. Red arrow indicates hypersignal from lentivirus infusion. **Middle panel.** PET signal of expression visualized with [11C]CLZ. White arrow indicates signal above background in the amygdala. **Right panel.** PET signal of expression visualized with [11C]DCZ. White arrow indicates signal above background in the amygdala. (For interpretation of the references to color in this figure legend, the reader is referred to the Web version of this article.)

ligands resulted in a strong signal throughout the left amygdala of the monkey, but the signal is better for [11C]DCZ (Fig. 7).

4. Discussion

In this study, we provided evidence that individual injections of a 20 µl suspension of lentivirus at a titer of 2×10^9 iu/ml can result in high efficiency transduction, without damage in confined regions of the old-world monkey amygdala. Multiple injections can be combined to target specific subnuclei and potentially the entire amygdala. The virus suspension can be mixed with the MRI markers Gadolinium or $MnCl_2$ and is stable at room temperature between 30 min and 8 h, making long infusions of the virus feasible without loss of efficacy. In addition, we showed that this strategy results in strong expression of the hM4Di_CFP chemogenetic receptor that can be visualized in the living monkey using [C11] PET ligands.

One of the goals of this study was to find an injection volume for lentivirus suspensions that results in good coverage but does not damage neuronal function. For AAV, large volumes had previously been injected into the striatum or Thalamus via convection enhanced delivery (CED) without causing much damage (Fiandaca et al., 2009). Lentivirus particles are larger than AAV particles (100 nm vs 20 nm) (Lentz et al., 2012), encountering more resistance diffusing through tissue. As we have shown here as well, expression of lentivirus is in general well confined, but also requires much higher volumes to cover equivalent regions compare to AAV (Lerchner et al., 2014). Lentivirus does not appear to have the same limited tropism, in terms of neuronal subtypes, as many AAVs (Lentz et al., 2012). Lentivirus has more uniform expression levels between neighboring neurons (Lerchner et al., 2023). Higher resistance to penetration may also result in higher local uptake of virus, which could explain the shutdown of NeuN expression seen in regions of high hM4Di_CFP expression close to the needle track of the 80 µl injection. We did not observe such NeuN shut-down with any of the 20 µl injections. While we don't know whether intermediate volumes would have resulted in such damage, we consider 20 µl a good compromise for regional coverage and preserving neuronal function in the tissue.

In the amygdala, all injections resulted in irregularities of regional coverage, i.e. we didn't observe spherical patterns of expression centered on the injection site. It has been previously shown that virus suspensions can travel along blood vessels (Lentz et al., 2012). In addition, it is possible that the structure of the amygdala – comprising multiple discrete subnuclei - contributes to the uneven distribution. On a practical level this means that if comprehensive coverage of a specific region is required, it may be necessary to take local sub-structure into account when planning injection patterns.

With multiple injections into a specific brain region, there is the increased possibility of needle blockage or mis-targeting of injections. One suggestion for mitigating the impact of needle blockages is to do a flow check each time the needle is removed from the brain. Here, we additionally used the MRI marker $MnCl_2$ to visualize injection of the virus suspension post-surgery (Lerchner et al., 2023; Fredericks et al., 2020). This turned out to be important when several of our injections appeared to fail (Fig. 5) and we were able to place additional injections in a subsequent surgery. Blockage of the needle may have been partly caused by precipitation of virus particles by the $MnCl_2$. Similar, issues with virus precipitation have been seen with another MRI marker Gal-bumin (Osting et al., 2014). In our lentivirus titer time course experiment, we showed that addition of up to 10 mM $MnCl_2$ did not result in additional degradation of the titer over time. For the lentivirus injections to bilaterally cover the amygdala, we had reduced the concentration of MnC_2 to 1 mM and still observed a strong hypersignal (Fig. 5A). More recently, we are using 0.1–0.2 mM $MnCl_2$ to better estimate the spread of the virus, and to allow the visualization of individual injection sites within a track (Fredericks et al., 2020). We also let the virus suspension equilibrate to room temperature before adding the $MnCl_2$. Together, these adjustments appear to have minimized issues with precipitation of lentivirus and $MnCl_2$ in our hands.

We achieved good, but by no means perfect coverage of the amygdala when we increased the number of injections to 12. In that experiment (Figs. 5 and 6), local neuronal penetrance of individual injections was not quantified but visually appeared as high as with our initial 20 µl injections but overall coverage of regions was less extended than expected. A reason for the lower-than-expected coverage in the more ventral/medial regions was likely that our injection tracks ended up more dorsal than originally intended (see Fig. 5A). Another possible reason is the distribution of injection sites. Each tract contained two or three injections at various depths, while the injections at the previous experiments were placed at a single depth. There was a clear difference in subnuclei coverage between the two hemispheres. For example, the left lateral basal amygdala showed a coverage of nearly 70% (LB – Fig. 6A) but the right lateral basal amygdala showed coverage in only 33% of the volume (LB – Fig. 6B). We observed no systematic bias in coverage, nor any apparent exclusion of cell types in either hemisphere. We previously showed that the human synapsin promoter used to drive reporter expression in this experiment is specific to neurons (Lerchner et al., 2014). Our current experiments were consistent with this result. Even in regions with up to 100% neuronal coverage, expression of the hM4Di_CFP reporter appeared to tightly correlate with cells also positive for the neuron maker NeuN (Fig. 2). As this pilot experiment was only done in a single monkey, and we did not stain for specific neuronal cell types, biased expression within neuronal cell populations cannot be excluded. In hindsight, dorsal bias and differences in injection locations are also confirmed by the Mn^{2+} hypersignal. Nonetheless, we believe our results show that it is possible to cover large and complex brain regions like the amygdala and achieve high neuronal transduction, even though more optimizations may be required.

Finally, we re-presented results from a previously published study (Yan et al., 2021), that used the injection strategy discussed here, to show that expression of the hM4Di_CFP chemogenetic receptor resulting from 20 µl injections is sufficiently high to produce a robust PET signal that can be detected in the living monkey.

Author contributions

WL conceived and coordinated all phases of the study. KD and DR imaged, analyzed and visualized amygdala histological data. KD, MAGE, WL conducted and analyzed lentivirus data, MAGE, KMR, VDC designed and conducted surgeries and MRI Formal analysis. XF prepared the PET figure from experiments previously published in (Yan et al., 2021). BA supervised the bilateral amygdala injection study. BJR supervised all phases of the study.

Declaration of competing interest

None.

Data availability

Full dataset can be accessed at: Mendeley Data, V1, doi: 10.17632/x8jh23yzvb.1

Acknowledgements

Appendix A. Supplementary data

Supplementary data to this article can be found online at https://doi.org/10.1016/j.crneur.2023.100091.

References

Eldridge, M.A., Lerchner, W., Saunders, R.C., Kaneko, H., Krausz, K.W., Gonzalez, F.J., Ji, B., Higuchi, M., Minamimoto, T., Richmond, B.J., 2016. Chemogenetic disconnection of monkey orbitofrontal and rhinal cortex reversibly disrupts reward value. Nat. Neurosci. 19, 37–39.

Fiandaca, M.S., Varenika, V., Eberling, J., McKnight, T., Bringas, J., Pivirotto, P., Beyer, J., Hadaczek, P., Bowers, W., Park, J., Federoff, H., Forsayeth, J., Bankiewicz, K.S., 2009. Real-time MR imaging of adeno-associated viral vector delivery to the primate brain. Neuroimage 47 (Suppl. 2), T27–T35.

Fredericks, J.M., Dash, K.E., Jaskot, E.M., Bennett, T.W., Lerchner, W., Dold, G., Ide, D., Cummins, A.C., Der Minassian, V.H., Turchi, J.N., Richmond, B.J., Eldridge, M.A.G., 2020. Methods for mechanical delivery of viral vectors into rhesus monkey brain. J. Neurosci. Methods 339, 108730.

Grayson, D.S., Bliss-Moreau, E., Machado, C.J., Bennett, J., Shen, K., Grant, K.A., Fair, D. A., Amaral, D.G., 2016. The rhesus monkey connectome predicts disrupted functional networks resulting from pharmacogenetic inactivation of the amygdala. Neuron 91, 453–466.

Guselnikova, V.V., Korzhevskiy, D.E., 2015. NeuN as a neuronal nuclear antigen and neuron differentiation marker. Acta Naturae 7, 42–47.

Janak, P.H., Tye, K.M., 2015. From circuits to behaviour in the amygdala. Nature 517, 284–292.

Jazayeri, M., Lindbloom-Brown, Z., Horwitz, G.D., 2012. Saccadic eye movements evoked by optogenetic activation of primate V1. Nat. Neurosci. 15, 1368–1370.

Kalin, N.H., Fox, A.S., Kovner, R., Riedel, M.K., Fekete, E.M., Roseboom, P.H., Trompo, P.M., Grabow, B.P., Olsen, M.E., Brodsky, E.K., McFarlin, D.R., Alexander, A.L., Emborg, M.E., Block, W.F., Fudge, J.L., Oler, J.A., 2016. Overexpressing corticotropin-releasing factor in the primate amygdala increases anxious temperament and alters its neural circuit. Biol. Psychiatr. 80, 345–355.

Kim, J., Zhang, X., Muralidhar, S., LeBlanc, S.A., Tonegawa, S., 2017. Basolateral to central amygdala neural circuits for appetitive behaviors. Neuron 93, 1464–1479 e1465.

Lentz, T.B., Gray, S.J., Samulski, R.J., 2012. Viral vectors for gene delivery to the central nervous system. Neurobiol. Dis. 48, 179–188.

Lerchner, W., Corgiat, B., Der Minassian, V., Saunders, R.C., Richmond, B.J., 2014. Injection parameters and virus dependent choice of promoters to improve neuron targeting in the nonhuman primate brain. Gene Ther. 21, 233–241.

Lerchner, W., Luz-Ricca, A., Dash, K., DerMinassian, V., Richmond, B.J., 2023. Production, testing, and verification of lentivirus for regional targeting in the old-world monkey brain. In: Eldridge, M.A.G., Galvan, A. (Eds.), Vectorology for Optogenetics and Chemogenetics. Springer US, New York, NY, pp. 3–15.

Lin, S.P., Brown, J.J., 2007. MR contrast agents: physical and pharmacologic basics. J. Magn. Reson. Imag. 25, 884–899.

Murray, E.A., Fellows, L.K., 2022. Prefrontal cortex interactions with the amygdala in primates. Neuropsychopharmacology 47, 163–179.

Nagai, Y., Kikuchi, E., Lerchner, W., Inoue, K., Ji, B., Eldridge, M.A.G., Kaneki, H., Kimura, Y., Oh-Nishi, A., Hori, Y., Kato, Y., Hirabayashi, T., Fujimoto, A., Kumata, K., Zhag, M., Aoki, I., Suhara, T., Higuchi, M., Takada, M., Richmond, B.J., Minamimoto, T., 2016. PET imaging-guided chemogenetic silencing reveals a critical role of primate rostromedial caudate in reward evaluation. Nat. Commun. 7, 13605.

Osting, S., Bennett, A., Power, S., Wackett, J., Hurley, S.A., Alexander, A.L., Agbandje-Mckena, M., Burger, C., 2014. Differential effects of two MRI contrast agents on the integrity and distribution of rAAV2 and rAAV5 in the rat striatum. Mol Ther Methods Clin Dev 1, 4.

Oyama, K., Hori, Y., Mimura, K., Nagai, Y., Eldridge, M.A.G., Saunders, R.C., Miyakawa, N., Hirabayashi, T., Hori, Y., Inoue, K.I., Suhara, T., Takada, M., Higuchi, M., Richmond, B.J., Minamimoto, T., 2022. Chemogenetic disconnection between the orbitofrontal cortex and the rostromedial caudate nucleus disrupts motivational control of goal-directed action. J. Neurosci. 42, 6267–6275.

Phelps, E.A., LeDoux, J.E., 2005. Contributions of the amygdala to emotion processing: from animal models to human behavior. Neuron 48, 175–187.

Raper, J., Murphy, L., Richardson, R., Romm, Z., Kovacs-Balint, Z., Payne, C., Galvan, A., 2019. Chemogenetic inhibition of the amygdala modulates emotional behavior expression in infant rhesus monkeys. eNeuro 6.

Roozendaal, B., McEwen, B.S., Chattarji, S., 2009. Stress, memory and the amygdala. Nat. Rev. Neurosci. 10, 423–433.

Roseboom, P.H., Mueller, S.A.L., Oler, J.A., Fox, A.S., Riedel, M.K., Elam, V.R., Olsen, M. E., Gomez, J.L., Boehm, M.A., DiFilippo, A.H., Christian, B.T., Michaelides, M., Kalin, N.H., 2021. Evidence in primates supporting the use of chemogenetics for the treatment of human refractory neuropsychiatric disorders. Mol. Ther. 29, 3484–3497.

Simmons, J.M., Saad, Z.S., Lizak, M.J., Ortiz, M., Koretsky, A.P., Richmond, B.J., 2008. Mapping prefrontal circuits in vivo with manganese-enhanced magnetic resonance imaging in monkeys. J. Neurosci. 28, 7637–7647.

Wank, I., Pliota, P., Badurek, S., Kraitsy, K., Kaczanowska, J., Griessner, J., Kreitz, S., Hess, A., Haubensak, W., 2021. Central amygdala circuitry modulates nociceptive processing through differential hierarchical interaction with affective network dynamics. Commun Biol 4, 732.

Yan, X., Telu, S., Dick, R.M., Liow, J.S., Zanotti-Fregonara, P., Morse, C.L., Manly, L.S., Gladding, R.L., Shrestha, S., Lerchner, W., Nagai, Y., Minamimoto, T., Zoghbi, S.S., Innis, R.B., Pike, V.W., Richmond, B.J., Eldridge, M.A., 2021. [(11)C] deschloroclozapine is an improved PET radioligand for quantifying a human muscarinic DREADD expressed in monkey brain. J. Cerebr. Blood Flow Metabol. 41, 2571–2582.

Zhao, K., Yan, W.J., Chen, Y.H., Zuo, X.N., Fu, X., 2013. Amygdala volume predicts inter-individual differences in fearful face recognition. PLoS One 8, e74096.